Tumor Biol. (2016) 37:9411–9422
DOI 10.1007/s13277-016-4824-5

ORIGINAL ARTICLE

Gastric cardia adenocarcinoma microRNA profiling in Chinese patients

Shegan Gao[1] · Fuyou Zhou[2] · Chen Zhao[3] · Zhikun Ma[1] · Ruinuo Jia[1] · Shuo Liang[1] · Mengxi Zhang[1] · Xiaojuan Zhu[1] · Pengfei Zhang[1] · Lu Wang[4] · Feng Su[4] · Jiangman Zhao[4] · Gang Liu[1] · Bo Peng[4] · Xiaoshan Feng[1,5]

Received: 23 October 2015 / Accepted: 8 January 2016 / Published online: 18 January 2016

Abstract Gastric cardia adenocarcinoma (GCA), which occurs at the gastroesophageal boundary, is one of the most malignant types of cancer. Over the past 30 years, the incidence of GCA has increased by approximately sevenfold, which has a more substantial increase than that of many other malignancies. However, as previous studies mainly focus on non-cardia gastric cancer, until now, the mechanisms behind GCA remain largely unknown. MicroRNAs (miRNAs) have been shown to play pivotal roles in carcinogenesis. To gain insight into the molecular mechanisms regulated by miRNAs in GCA development, we investigated miRNA expression profiles using 81 pairs of primary GCAs and corresponding non-tumorigenic tissues. First, 21 pairs of samples were used for microarray analysis, and then another 60 pairs of samples were used for further analysis. Our results showed that 464 miRNAs (237 upregulated, 227 downregulated, false discovery rate FDR <0.05) were differently expressed between GCA and non-tumor tissues. Pearson test and pathway analysis revealed that these dysregulated miRNA correlated coding RNAs may have effects on several cancer-related pathways. Four miRNAs (miR-1244, miR-135b-5p, miR-3196, and miR-628-3p) were found to be associated with GCA differentiation. One miRNA, miR-196a-5p, was found to be associated with age of GCA onset. Further, survival analysis showed that the expression level of miR-135b-5p was associated with GCA survival. Taken together, our study first provided the genome-wide expression profiles of miRNA in GCA and will be good help for further functional studies.

Keywords microRNA · Microarray · Gastric cardia adenocarcinoma · Differentiation · miR135b-5p

Shegan Gao, Fuyou Zhou and Chen Zhao contributed equally to this work.

Electronic supplementary material The online version of this article (doi:10.1007/s13277-016-4824-5) contains supplementary material, which is available to authorized users.

✉ Bo Peng
bpeng@biotecan.com

✉ Xiaoshan Feng
samfeng137@hotmail.com

[1] Henan Key Laboratory of Cancer Epigenetic; Cancer Institute, The First Affiliated Hospital, and College of Clinical Medicine of Henan University of Science and Technology, Luoyang, China, 471003, Luoyang 471003, China

[2] Department of Oncology, Anyang People's Hospital, Anyang 471500, China

[3] Fudan-Zhangjiang Center for Clinical Genomics, Zuchongzhi Road 899, Shanghai 201203, China

[4] Zhangjiang Center for Translational Medicine, Zuchongzhi Road 899, Shanghai 201203, China

[5] Henan University of Science and Technology, Jing hua Road 24, Luoyang 471500, China

Introduction

Gastric cardia cancer (GCC), which occurs in the 1-cm (cm) proximal and 2-cm distal region of the esophagogastric junction, is one of the most fetal tumors [1]. The predominant histological type of GCC is gastric cardia adenocarcinoma (GCA). In the last 30 years, incidence of GCA has raised about sevenfold, which has a more substantial increase than that of several other malignancies [2–5]. There is an urgent need to understand the mechanisms involved in GCA as well as to elucidate early diagnosis and prognostic biomarkers associated with GCA to discover new strategies for controlling this type of cancer.

The Henan province of China is an area with the highest GCA incidence rate in the world, 190/1,000,000, and this rate is still increasing [6]. Previous studies have identified several risk factors associated with GCA development, including lifestyle factors (smoking, consuming irritating drinks, eating irregularly) and disease conditions (obesity, gastrointestinal inflammation, gastroesophageal reflux, Helicobacter pylori infection) [7, 8]. However, as investigations focus predominantly on non-cardia gastric adenocarcinoma (GA) samples, molecular data for GCA samples remains very limited.

The discovery of non-coding RNAs (ncRNAs) represented a milestone in molecular biology. Generally, ncRNAs can be grouped into two major classes: small ncRNAs and long ncRNAs (lncRNAs) [9, 10]. MicroRNAs (miRNAs) are a class of single-stranded, small (20–22 nt) ncRNAs that regulate a wide range of biological processes, such as development, cell growth, signal transduction, and apoptosis [9, 10]. Generally, a single miRNA can regulate multiple mRNAs, and a single mRNA may be regulated by numerous miRNAs [9, 10]. Recently, miRNA expression has been examined via microarray or other non-high throughput technologies. These miRNA studies have indicated that miRNAs might be involved in many known oncogenic pathways, such as the Wnt, P53, or K-ras pathways [9–11]. In addition, dysregulation of miRNA expression has been frequently observed in different types of cancer [11–15].

miRNA profiling in non-cardia GA has been previously reported [16, 17], but few studies have focused on GCA. In the present study, we used microarray analysis to explore the genome-wide miRNA expression profile of 21 pairs of GCA and matched normal cardia tissues and used quantitative RT-PCR to investigate the relationship between several dysregulated miRNAs and clinicopathological characteristics in another 60 pairs of GCA and matched normal cardia tissues. This investigation aimed to provide resources for understanding the role of miRNA in GCA.

Materials and methods

Samples

Cardia carcinoma and normal cardia tissue used for microarray analysis were obtained from 21 patients who underwent surgical resection at the First Hospital Affiliated to Henan University of Science and Technology between November and December in 2012. Twelve pairs of these samples were also used for mRNA microarray analysis in our previous published data [18]. Another 60 paired tissue samples used for association analysis and survival analysis were from two hospitals: the First Affiliated Hospital of Henan University of Science and Technology and the AnYang Cancer Hospital affiliated to Henan University of Science and Technology. All the patients included in this research had not received adjuvant chemotherapy before surgery. The tissue samples, including GCA tissues and non-tumor matches, were flash-frozen in liquid nitrogen during surgery and then stored at −80 °C until RNA extraction. The anatomical sites of the primary GCAs were from the dentate line of the gastroesophageal junction to 2 cm below that line. Adjacent non-cancerous tissue matches were collected with a minimum of 1 cm. Both tumor and non-tumor matches were confirmed by histological examination. Tumor stage was evaluated according to the seventh edition of the American Joint Committee on Cancer TNM staging system. The patient characteristics are described in Table 1. This study was approved by the institutional review board of the hospital (IRB no. 2013-002). Written informed consent was obtained from the patients before surgery.

MicroRNA microarray analysis

Total RNA from 21 pairs of specimens was extracted using TRIzol (Life Technologies, Carlsbad, CA) and reverse transcribed using a PrimeScript RT Reagent Kit. The samples were labeled using a MiRCURY Array Hy3/Hy5 Power Labeling Kit (Cat no. 208032-A, Exiqon, Vedbaek, Denmark) and hybridized on a MiRCURY Array (Exiqon, Vedbaek, Denmark). After the hybridization reaction, the arrays were scanned using an Axon GenePix 4000B microarray scanner

Table 1 Clinicopathological characteristics of the patients

Characteristics	No. of patients (microarray analysis)	No. of patients (qPCR validation and association analysis)
Age (years)		
≤60	12	24
>60	9	36
Differentiation		
Poor	9	31
Moderate	10	20
Well	2	9
Invasion status		
Yes	21	60
No	0	0
Lymphatic metastasis		
Yes	16	49
No	5	11
TNM stage		
I	0	0
II	3	15
III	18	43
IV	0	2

(Axon Instruments, Foster City, CA). The raw intensity image was analyzed using GenePix Pro v6.0 software.

Microarray data analysis

The median normalization method was used to obtain "normalized data" (normalized data = (foreground-background) / median). The median is 50 % quantile of microRNA intensity which is larger than 30 in all samples after background correction. The statistical significance of differentially expressed miRNAs was analyzed by *t* test.

Detection of miRNAs by real-time RT-PCR

miRNAs were isolated from 60 paired GCA and adjacent non-tumor tissue samples using a miRNeasy Mini Kit (Qiagen, Hilden, Germany) according to the manufacturer's instructions. cDNA synthesis and miRNA amplification were performed using an All-in-One™ miRNA qRT-PCR Detection Kit (GeneCopoeia, Rockville, MD, USA), and all the miRNA primers used in this study were purchased from GeneCopoeia (Rockville, MD, USA). PCR was performed using a Bio-Rad CFX96 Real-Time PCR instrument (Bio-Rad, CA, USA). The relative expression of select mature miRNAs in GCA and adjacent non-tumor tissues was obtained using the comparative CT method ($2^{-\Delta\Delta CT}$). U6 snRNA expression was used as the endogenous control to normalize the data.

Cell lines and plasmids

Two cell lines, OE-19 and SK-GT2, originating from esophageal gastric junction, were bought from The European Collection of Cell Cultures (ECACC). Both cell lines were cultured in RPMI1640 supplemented with 10 % fetal bovine serum. miR135b-5p expression and inhibition plasmids were bought from GeneCopoeia, using pEZX-MR03 vector and pEZX-AM03 vector respectively.

Colony formation assay and cell proliferation assay

For colony formation assay, cells with 60 % confluency were transfected with miR-135b-5p expression or inhibition plasmids using Lipofectamine 2000 (Invitrogen). Twenty-four hours later, we observed these cells under fluorescence microscope. If the transfection efficiency among expression plasmid, inhibition plasmid, and their control vectors were comparable, we then portioned cells into 6-well plate at the density of 3000/well in triplicate. Puromycin or hygromycin was added into the medium 24 h later. After about 10-day culture, colonies were identified by crystal violet staining. For cell proliferation assay, cells with 60 % confluency were transfected with miR-135b-5p expression or inhibition plasmids using Lipofectamine 2000 (Invitrogen). Twenty-four hours later, we observed these cells under fluorescence microscope. If the transfection efficiency among expression plasmid, inhibition plasmid, and their control vectors were comparable, we then portioned cells into 96-well plate at the density of 2000 each well. Puromycin or hygromycin was added into the medium. Then, cells were subjected to the CCK-8 assay (Dojindo) during the next 6 days. Cell growth curve was expressed at the absorbance at 490 nm ($n = 6$), which was read by a microtiter reader (Bio-Rad).

miRNAs and mRNA correlation analysis and pathway analysis

We conducted Pearson test to identify miRNA-correlated mRNAs using microarray data from 12 out of 21 samples. These 12 samples were used for miRNA microarray analysis and mRNA microarray analysis at the same time. The mRNA microarray data were published in our previous paper [18]. Significantly differentially expressed miRNAs and mRNAs were selected for correlation analysis. R software was used (version 2.15.2). Pathway analysis of miRNA-correlated mRNAs (absolute value of $R^2 > 0.6$) was conducted using ingenuity pathway analysis (IPA; http://www.ingenuity.com/products).

Statistical analysis

SPSS version 18.0 (SPSS Inc. Chicago, IL, USA) was used to conduct the statistical analysis, except for microarray analysis and Pearson test, where R was used. The associations between miRNA expression and clinicopathological characteristics, including gender, age, TNM stage, differentiation status, and lymph node metastasis, were assessed using *t* test or ANOVA. Univariate analysis was used to explore clinicopathologic parameters related with overall survival (OS, the time from the date of primary surgery to the date of death). Then Kaplan-Meier survival analysis was applied to test the correlations between the miRNA expression level and patients' overall survival, and log-rank test was performed to test the statistical differences between survival curve of patients with different miRNA expression levels. For all the tests and comparisons, a value of $p < 0.05$ (*) was considered statistically significant.

Results

Identification of altered miRNA expression in GCA

A total of 21 pairs of GCA and matched adjacent non-tumor tissues measuring a minimum of 1 cm were collected for this

study. The tissue samples were flash-frozen in liquid nitrogen during resection and then stored at −80 °C until RNA extraction. The study population consisted of 17 males and 4 females, with a median age of 60 years old (range 42–79 years). All the GCA tissues were histopathologically confirmed. The details of patient characteristics were listed in Table 1. Microarray analysis of 21 pairs of tumor and non-tumor tissue samples was conducted at the same time. Before calculating the miRNA expression levels, we analyzed the spike-in probes in each chip using the raw data. Two pairs of samples were excluded because the spike-in probe analysis revealed that the coefficient of variation was greater than 0.2 or the correlation coefficient was less than 0.6.

By comparing the miRNA expression levels in a total of 19 primary GCA and matched non-tumor tissues, we identified 237 upregulated miRNAs and 227 downregulated miRNAs (FDR < 0.05) (Table 2, Supplementary Table 1). Hsa-miR-196a-5p and hsa-miR-3656 were the most upregulated and downregulated miRNAs, respectively (Table 2). Hierarchical clustering analysis was conducted to group the specimens according to expression level (Fig. 1a). Among dysregulated miRNAs, certain miRNAs have been proved dysregulated in tumors by previous studies, such as hsa-miR-148a-3p [19], hsa-miR-196a-5p [20], and hsa-miR-20a-5p [21].

Real-time quantitative PCR validation

To confirm the expression levels of the identified miRNAs by microarray, we randomly selected eight upregulated and eight downregulated miRNAs for qPCR validation. The qPCR results were consistent with microarray results. Then, we focused on 6 dysregulated miRNAs and used another 60 pairs of GCA samples obtained from the First Hospital and the AnYang Cancer Hospital affiliated to Henan University of Sciences and Technology. Hsa-miR-135b-5p, hsa-miR-196a-5p, and has-miR-1244 expression was increased, whereas hsa-miR-628-3p, hsa-miR-148a-3p, and hsa-miR-3196 expression was decreased in the GCA samples compared with the matched normal samples (Fig. 1b). The qPCR results were consistent with the microarray data.

miRNA and mRNA correlation analysis and pathway analysis

In order to predict the function of dysregulated miRNAs, we identified their correlated coding RNAs. As 12 samples used for miRNA microarray analysis were also used for mRNA microarray analysis at the same time, we calculated the relationship between differentially expressed miRNAs and

Table 2 Top 20 significantly down and upregulated miRNAs

Downregulated miRNAs			Upregulated miRNAs		
miRNA	Fold change (log2)	*p* value	miRNA	Fold change (log2)	*p* value
hsa-miR-3656	−3.29535	1.89E−16	hsa-miR-196a-5p	4.111534	3.36E−14
hsa-miR-378c	−1.80765	8.96E−14	hsa-miR-135b-5p	2.555514	2.67E−13
hsa-miR-628-3p	−2.03238	2.23E−13	hsa-miR-2355-3p	1.517697	2.68E−13
hcmv-miR-US33-3p	−2.25544	2.67E−13	hsa-miR-4307	2.371521	1.05E−09
hsa-miR-148a-3p	−1.63085	2.67E−13	hsa-miR-1244	2.409671	3.68E−09
hsv2-miR-H10	−2.84551	4.43E−13	hsa-miR-892a	1.8554	1.05E−08
hsa-miR-638	−1.55968	8.99E−13	hsa-miR-20a-5p	1.501549	1.15E−08
hsa-miR-483-5p	−1.35334	2.20E−12	hsa-miRPlus-A1087	2.115592	6.38E−08
hsa-miR-675-5p	−1.70156	5.11E−12	hsa-miR-93-5p	1.5392	1.06E−07
hsa-miR-1184	−1.00147	2.67E−11	hsa-miR-455-3p	1.568063	1.80E−07
hsa-miR-299-5p	−1.66357	3.05E−11	hsa-miR-105-5p	1.755387	1.96E−07
hsa-miR-4285	−1.06365	4.74E−11	hsa-miR-764	1.650002	2.58E−07
hsa-miR-3665	−1.95478	9.57E−11	hsa-miR-130b-5p	1.660447	4.98E−07
hsv2-miR-H25	−1.61128	1.04E−10	hsa-miR-506-3p	1.605885	2.66E−06
hsv1-miR-H17	−1.53334	1.41E−10	hsa-miR-454-3p	1.515466	3.92E−06
hsa-miR-3195	−1.28305	1.41E−10	hsa-miR-142-3p	1.524762	4.35E−06
hsa-miR-518e-5p	−0.97021	1.41E−10	hsa-miR-3591-3p	1.452323	1.19E−05
hsa-miR-3196	−2.64801	7.06E−10	hsa-miR-196b-5p	1.682773	1.67E−05
hsa-miR-30d-5p	−0.74407	7.06E−10	hsa-miR-3664-5p	1.737875	4.36E−05
hsa-miR-3124-5p	−2.60563	2.21E−09	hsa-miR-636	1.557929	9.98E−05

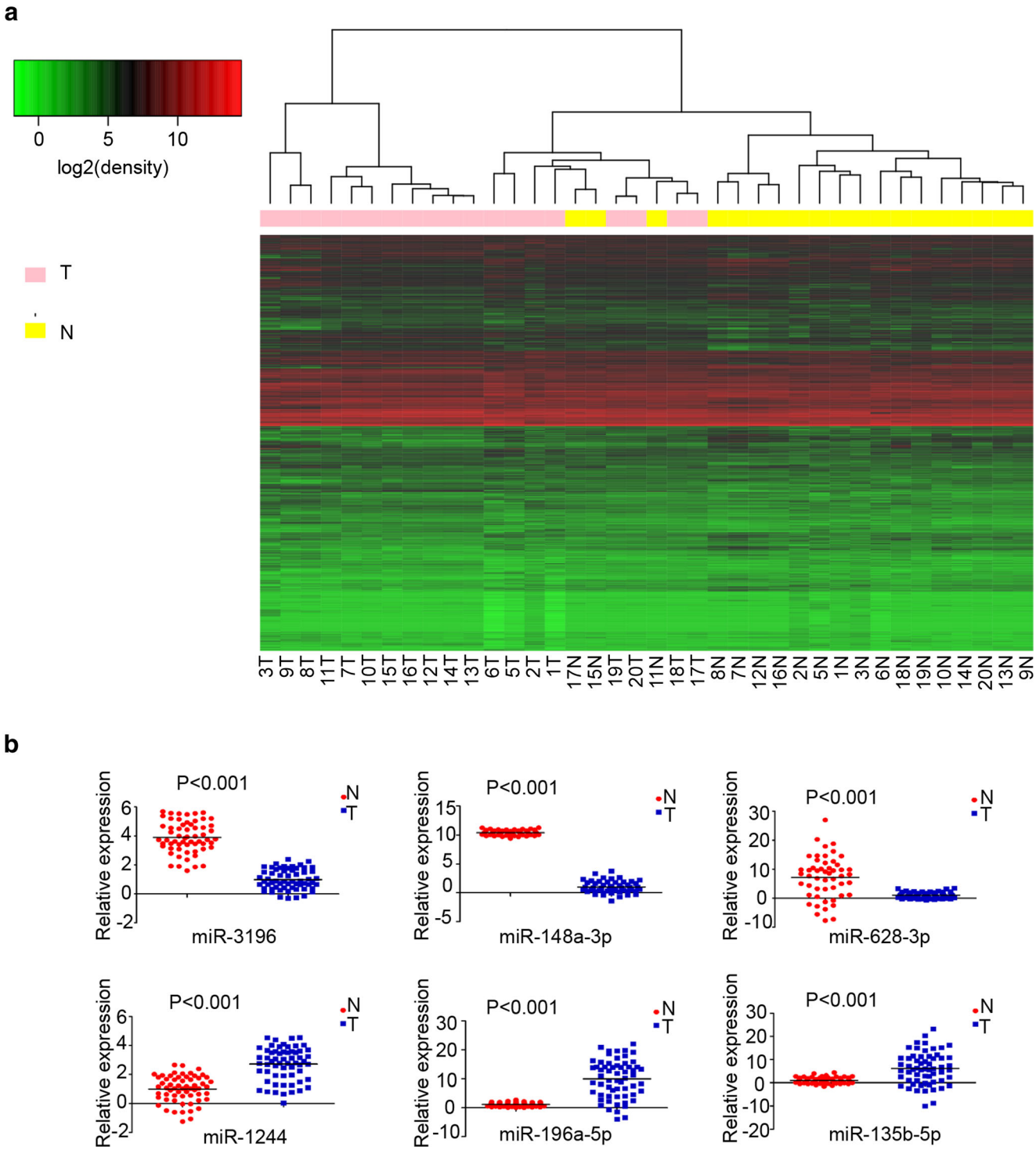

Fig. 1 Hierarchical clustering dendrogram and validation results. **a** Analysis of 19 pairs of miRNA chips using a heat map. The hierarchical clustering analysis was performed by all the miRNAs in the microarray to show the difference of miRNA expression profiles between tumor and normal tissues. **b** Microarray validation experiments using quantitative RT-PCR. The different expression of six miRNAs in GCA compared to normal tissue was validated. Each value represents the relative expression calculated using the comparative CT method with U6 snRNA as the endogenous control

mRNAs using microarray data from these 12 samples. In all, 1057 and 1249 correlated mRNAs were identified for upregulated and downregulated miRNAs, respectively.

Then, we input the miRNA-correlated mRNAs into the IPA system for pathway analysis. the top three pathways corresponding to the upregulated miRNA-correlated

mRNAs were EIF2 signaling ($p = 4.85E{-}8$), antigen presentation pathway ($p = 6.44E{-}4$), and phagosome maturation ($p = 6.59E{-}4$) (Fig. 2). The top three pathways corresponding to downregulated miRNA-correlated mRNAs were mTOR signaling ($p = 3.24E{-}5$), regulation of elf4 and p70S6K signaling ($p = 4.86E{-}5$), and mitochondrial dysfunction ($p = 1.14E{-}3$) (Fig. 2). Then, we carried out real-time PCR to validate two of the aforementioned

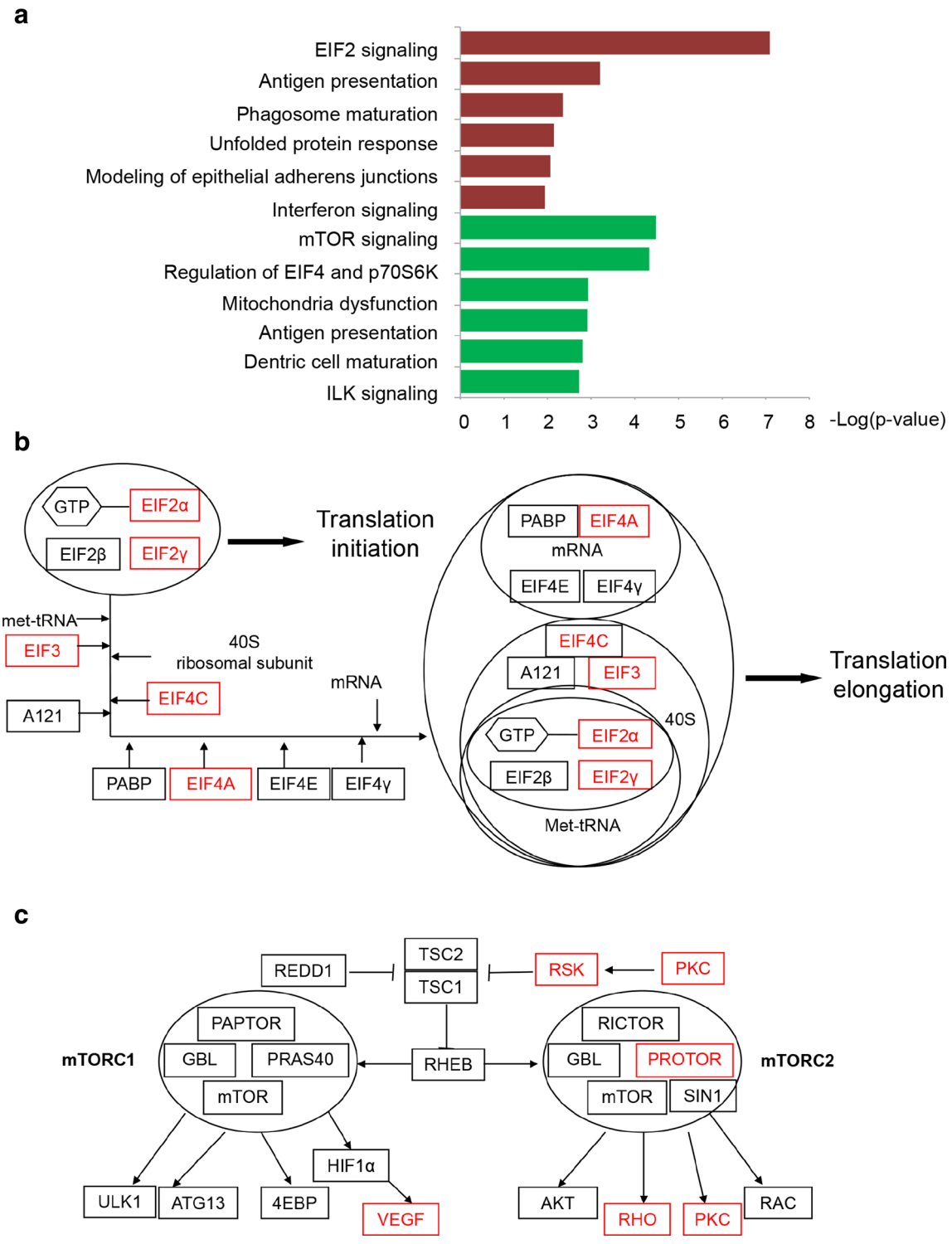

Fig. 2 Pathway analysis of dysregulated miRNA-correlated mRNAs. **a** Pathways corresponding to up (in *red color*) and down (in *green color*)-regulated miRNA-related mRNAs; **b**, **c** schematic diagram of pathway EIF2 and mTOR, respectively. The *word in red* represents the dysregulated miRNA-correlated mRNAs

pathways, EIF2 and mTOR, using 20 pairs of primary GCA and non-tumor matches. As shown in Supplementary Fig. S1, in most of GCA tissues, four important genes in the EIF2 pathway were upregulated and four important genes in the mTOR pathway were upregulated, indicating activation of these pathways in GCA.

Relationships between clinicopathological parameters and miRNA expression

To evaluate the clinical significance of the dysregulated miRNAs in GCA, we analyzed the relationships between six aforementioned miRNA expression levels in tumor tissues and clinicopathological parameters of the patients. These analyses revealed that the upregulation of miR-1244 was significantly correlated with better differentiation ($p = 0.007$), while upregulation of miR-135b-5p was correlated with poorer differentiation ($p = 0.009$). Downregulation of miR-3196 and miR-628-3p correlated with poor differentiation ($p = 0.018$ and $p = 0.044$, respectively) (Table 3, Supplementary Fig. S2). Higher miR-196a-5p expression levels were found in patients (36/60) older than 60 years of age, suggesting that miR-196a-5p could be associated with age of GCA onset (Table 3). However, miR-148a showed no correlation with differentiation status or age of GCA onset. In addition, analysis of other

Table 3 Associations between expression levels of miRNAs and clinicopathological features

	miR-196a-5p			miR-148a-3p			miR-1244		
	Total ($n = 60$)	Mean ± SD	p value	Total ($n = 50$)	Mean ± SD	p value	Total ($n = 59$)	Mean ± SD	p value
Gender			0.948			0.733			0.212
Male	44	7.67 ± 0.96		39	8.07 ± 0.37		43	7.59 ± 1.12	
Female	16	7.65 ± 1.21		11	8.11 ± 0.32		16	8.05 ± 1.48	
Age (year)			0.001			0.389			0.627
≤60	24	7.15 ± 0.86		21	8.13 ± 0.38		24	7.62 ± 1.21	
>60	36	8.01 ± 0.99		29	8.04 ± 0.33		35	7.78 ± 1.27	
TNM stage			0.636			0.313			0.467
II	15	7.54 ± 1.26		12	7.99 ± 0.28		15	7.92 ± 1.33	
III	45	7.71 ± 0.95		38	8.11 ± 0.37		44	7.65 ± 1.21	
Differentiation			0.27			0.634			0.007
Well	14	7.95 ± 1.53		5	8.04 ± 0.35		9	8.81 ± 0.98	
Moderate	20	7.25 ± 0.80		16	8.11 ± 0.37		19	7.67 ± 1.24	
Poor	26	7.67 ± 1.06		25	7.84 ± 0.67		26	7.41 ± 1.01	
Lymph node metastasis			0.79			0.746			0.901
Negative	11	7.56 ± 1.58		10	8.04 ± 0.29		11	7.67 ± 1.30	
Positive	49	7.69 ± 0.88		40	8.09 ± 0.37		48	7.73 ± 1.23	
	miR-3196			miR-135b-5p			miR-628-3p		
	Total ($n = 58$)	Mean ± SD	p value	Total ($n = 58$)	Mean ± SD	p value	Total ($n = 50$)	Mean ± SD	p value
Gender			0.232			0.865			0.493
Male	46	7.84 ± 0.91		46	7.59 ± 0.87		39	7.89 ± 0.70	
Female	12	7.48 ± 0.95		12	7.62 ± 0.63		11	7.72 ± 0.81	
Age (year)			0.653			0.107			0.478
≤60	23	7.83 ± 0.85		23	7.77 ± 0.68		21	7.94 ± 0.67	
>60	35	7.72 ± 0.98		35	7.48 ± 0.63		29	7.80 ± 0.76	
TNM stage			0.524			0.201			0.721
II	13	7.91 ± 0.98		13	7.80 ± 0.56		12	7.92 ± 0.83	
III	45	7.72 ± 0.92		45	7.54 ± 0.68		38	7.84 ± 0.69	
Differentiation			0.018			0.009			0.044
Well	7	8.51 ± 0.56		7	7.40 ± 0.53		5	8.61 ± 0.39	
Moderate	19	7.89 ± 0.93		19	7.46 ± 0.47		16	7.72 ± 0.68	
Poor	27	7.48 ± 0.86		27	7.96 ± 0.70		25	7.82 ± 0.73	
Lymph node metastasis			0.72			0.387			0.748
Negative	10	7.66 ± 1.02		10	7.76 ± 0.70		10	7.92 ± 0.95	
Positive	48	7.78 ± 0.91		48	7.56 ± 0.65		40	7.84 ± 0.66	

parameters revealed that these six miRNAs were not associated with gender, tumor stage, or lymph node metastasis.

Association between miRNA expression and patients' survival

To explore factors responsible for patients' survival, univariate analysis was conducted. Differentiation status was associated with GCA risk, while gender, age, TNM stage, and lymph node metastasis were not associated with GCA survival. Among the four differentiation-related miRNAs, miR135b-5p expression level is related to GCA survival. Furthermore, results of Kaplan-Meier plots and Log rank test showed that patients with low miR-135b-5p expression had a significantly better prognosis than those with high miR-135b-5p expression ($p = 0.043$). Maybe, because of the small sample size, expression level of miR-3196, miR-628, and miR-1244 exhibited no significant relationship with survival (Fig. 3).

miR-135b-5p prompting cell growth

As expression level of miR-135b-5p is related to patients' survival, we further examined the possible role of miR-135b-5p in cancer cell lines. First, we carried out colony formation assay. As shown in Fig. 4a, b, miR-135b-5p inhibition plasmid-transfected cells displayed a reduced number of colonies compared to control plasmid-transfected cells, while miR-135b-5p expression plasmid-transfected cells displayed an increased number of colonies compared to control plasmid-transfected cells.

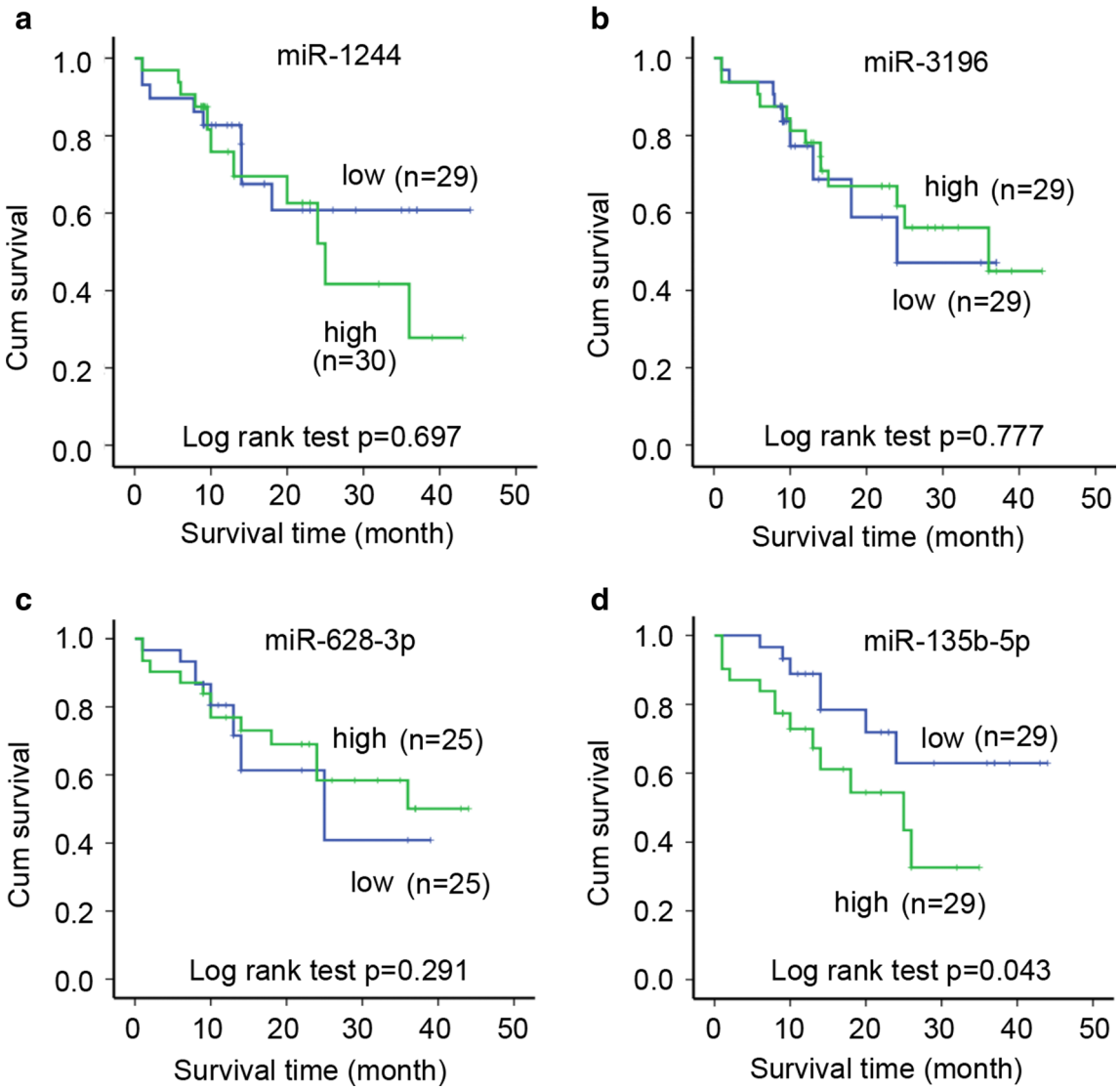

Fig. 3 Associations of four miRNA (**a** miR-1244, **b** miR-3196, **c** miR-628-3p, **d** miR-135b-5p) expression level with the overall survival of 60 GCA patients. RNA expression was grouped into low and high categories using the median as cutoff

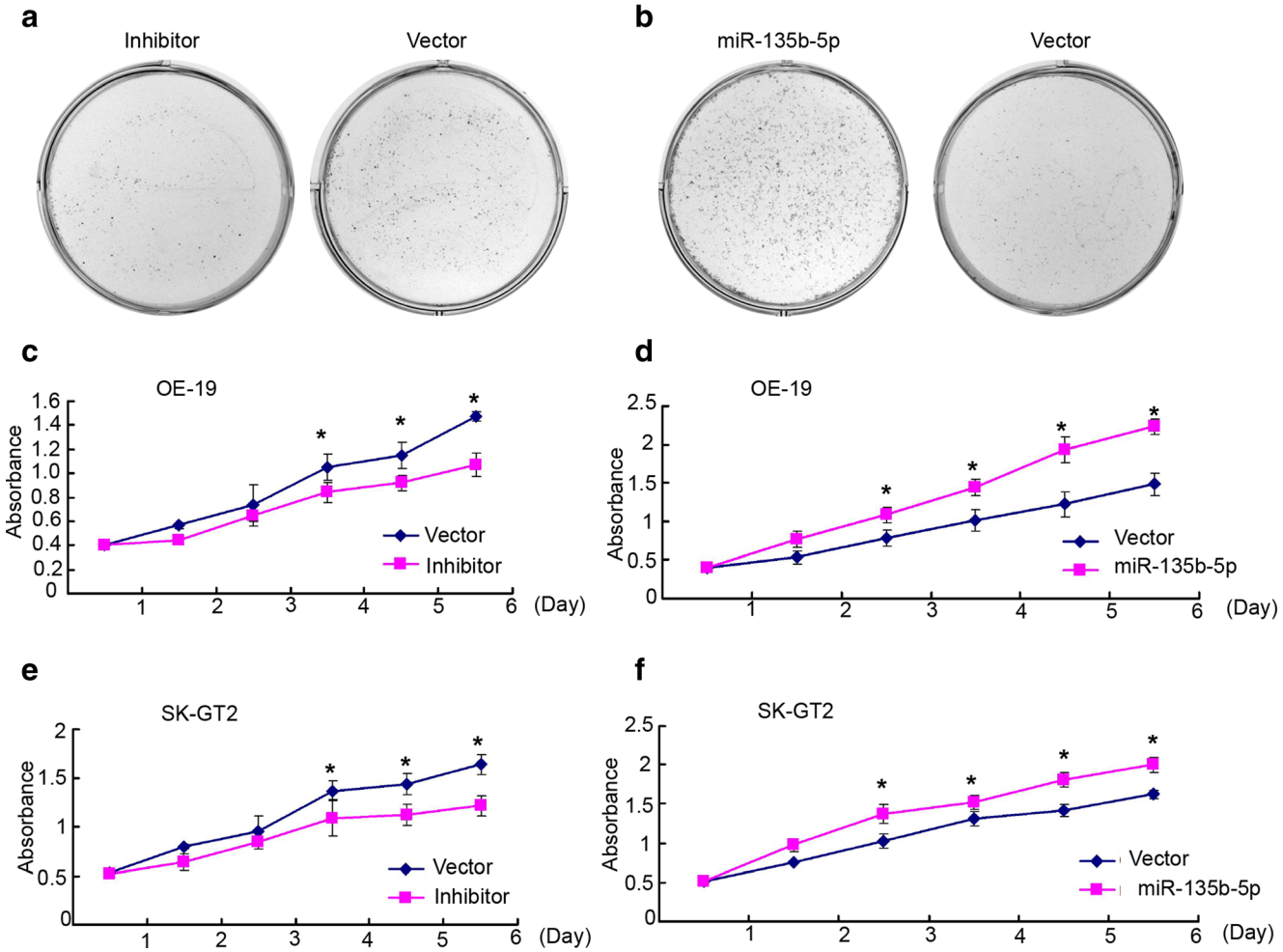

Fig. 4 miR-135b-5p prompting tumor cell malignancy. **a** knocking down miR-135b-5p in OE-19 inhibits colony formation; **b** overexpression of miR-135b-5p in OE-19 prompts colony formation; **c**, **e** knocking down miR-135b-5p inhibits cell growth; **d**, **f** overexpression of miR-135b-5p prompts cell growth. *$p < 0.01$

Then, we conducted cell proliferation assay. As shown in Fig. 4c–f, the growth rate of miR-135b-5p inhibition plasmid-transfected cells was significantly lower than that of control plasmid-transfected cells, while the growth rate of miR-135b-5p expression plasmid-transfected cells was significantly higher than that of control plasmid-transfected cells. Thus, these data suggest that miR-135b-5p could prompt cell growth.

Discussion

GCA morbidity and mortality rates have increased in recent years. There is an urgent need to understand the mechanisms involved in GCA as well as to elucidate diagnose and prognostic biomarkers associated with GCA to discover new strategies for controlling this type of cancer. miRNA profiling in cancer has received substantial attention because numerous miRNAs have been recognized to play critical roles in cancer progression and development. However, little is known regarding the miRNA profile of GCA. In the present study, we used microarray analysis to explore the genome-wide miRNA expression profiles in 21 primary GCA samples. It is the first time genome-wide miRNA expression profile in GCA is reported.

The results of microarray analysis revealed that there were 464 miRNAs that were significantly differentially expressed between the GCA tissue and paired non-cancerous matches (FDA < 0.05). In order to predict the function of dysregulated miRNAs, we identified the miRNA-correlated coding RNAs and conducted pathway analysis. For upregulated miRNA-correlated mRNAs, the most enriched pathway was EIF2 signaling. The translation initiation factor EIF2, composed of α, β, and γ, acts as an essential factor in global translation initiation of eukaryotic cells. The α subunit regulates the level of active EIF2 complex, the β subunit interacts with eukaryotic

translation initiation factors and mRNAs, and the γ-subunit binds to GTP or GDP [22, 23]. In translation initiation, EIF2 binds to methionyl-tRNA, 40S small ribosomal subunit, and recruited other initiation factors, forming initiation factor complex [22, 23]. Over the last decade, the function of the EIF2 pathway has been found to be of critical importance for promoting cellular adaptation and tolerance to stresses. As tumor grows in size, cancer cells have to respond to stress, such as hypoxia, low nutrient concentrations, and low pH in microenvironment, through the EIF2 pathway [24, 25]. Changes of expression level and phosphorylation status of EIF2 factors in tumor samples compared to matched normal tissues have been observed in different types of cancer [22, 24, 25]. These days, a number of small molecular weight compounds targeting the EIF2 pathway have been developed and may be potential therapy strategy in the future [22, 26]. Future studies should pay more attention on the role of EIF2 in the GCA. For downregulated miRNA-correlated mRNAs, the most enriched pathway was the mTOR pathway, which regulates a complex array of cellular functions in cancer, involving gene transcription, cell growth, proliferation, and survival [27, 28]. The mTOR pathway is restrained in normal cell, but is constitutively activated in cancers. mTOR functions to regulate the cellular signaling processes in two cellular complexes: mTOR complex 1 (mTORC1) and mTOR complex 2 (mTORC2). The two complexes differ in terms of subcellular localization, function, and regulation, and mTOR1 is more clearly understood [27, 28]. mTOR1 signaling can not only be activated by growth factor receptor signaling through the PI3K-AKT pathway but also by nutrient and energy status [28, 29]. Recently, mTORC1 inhibitors, such as everolimus, have been developed, investigated in patients with metastatic breast cancer [30], bladder cancer [31], and renal cell cancer [32], and has demonstrated improved patient outcomes. Our results indicated the important role of mTOR in GCA. If further studies validated the activation of mTOR in GCA, it would be good news for advanced GCA patients.

Our microarray analysis identified more than 400 dysregulated miRNAs; we focus six of them for further study and found that five miRNAs may represent a potential biomarker for clinicopathological parameters. miR-196a-5p expression level is observed to be associated with age of GCA onset, while four dysregulated miRNAs, miR-3196 miR-628-3p, miR-1244, and miR-135b-5p, were found to be related to GCA differentiation status. Previous studies have not only observed different expression levels of several of these miRNAs in cancer tissues compared with normal matches but also found the relationship between these miRNA expression level and clinicopathologic features. For example, miR-196 plays critical roles in normal development and in the pathogenesis of human disease processes such as cancer [33, 34]. Functionally, miR-196 performed their function by inhibiting NME4 expression and further activating p-JNK, suppressing TIMP1, augmenting MMP1/9, interacting with HOXB, HOXB targeting, and Sonic hedgehog (Shh) promoting proliferation of and suppressing apoptosis both in vitro and in vivo [35, 36]. miR-3196 is dysregulated in breast cancer and skin basal cell carcinoma, expression level of which was related to metastasis and other clinicopathological features [37–39].

Results of univariate analysis showed that differentiation status is related to patient survival. Log-rank analysis revealed that low expression level of miR-135b-5p is associated with better prognosis. miR-135-5p has been reported to be upregulated in different tumors, such as osteosarcoma and non-cardia GA. Only one functional validated target of it, DISC1, has been reported [40]. By Pearson test, miR-135-5p-related miRNAs have been identified, and several of them are in cancer-related pathways. For example, PARD3, TUBA1C, and TUBB2A are in the adherens junction signaling pathway; RPL1, RPL27, and RPs10 are in the EIF2 signaling pathway; and DUSP2, ELF4, and PPP2R2B are in the ERK/MAPK pathway. Further functional studies are needed to explain the mechanism behind miR-135-5p. Maybe because of small sample size, survival analysis showed no significant association of miR-3196, miR-628-3p, miR-1244, and patients with survival time; it is noteworthy for further studies with larger sample size to explore their role in GCA or in a certain GCA subtype.

To compare miRNA expression profile among esophageal, gastric, and cardiac cancer, we conducted a comparative analysis and found that GCA exhibited closer relationship with non-cardia gastric and esophageal adenocarcinoma but farther relationship with esophageal squamous cell carcinoma (ESCC) (data not shown). Similarly, Song et al. compared the genetic alteration characters among ESCC, esophageal adenocarcinoma (EAC), and head and neck squamous cell carcinoma (HNSCC) and found that ESCC genetic alteration was more similar to that in HNSCC than to that in EAC [41]. These studies indicated that molecular profile may be more closely related to histological type than to tumor-originating organs. As the public datasets for non-cardia gastric cancer or esophageal cancer were limited, it is a pity that we could not calculate whether gastric cardia adenocarcinoma is closer to non-cardia GA or EAC.

In conclusion, we explored miRNA expression profiles in 81 pairs of primary GCA samples. Our results showed that more than 400 miRNAs were differentially expressed between primary GCA and matched non-tumor tissues. These dysregulated miRNAs may have effects on several important cancer-related pathways. Furthermore, four miRNAs (miR-1244, miR-135b-5p, miR-3196, and miR-628-3p) were found to be associated with GCA differentiation. Expression level of

miR-135b-5p was associated with cancer survival. Our study first provided the genome-wide expression profiles of miRNA in GCA and will be of good help for further functional studies.

Acknowledgments This work was supported by the Natural Science Foundation of China (NSFC, 81472234, GSG).

The authors would like to thank Professor LemingShi (Center for Pharmacogenomics, State Key Laboratory of Genetic Engineering and MOE Key Laboratory of Contemporary Anthropology, Schools of Life Sciences and Pharmacy, Fudan University, Shanghai 201203, China) for data analysis.

Compliance with ethical standards

Conflicts of interests None

References

1. Chow WH, Blot WJ, Vaughan TL, Risch HA, Gammon MD, Stanford JL, et al. Body mass index and risk of adenocarcinomas of the esophagus and gastric cardia. J Natl Cancer Inst. 1998;90: 150–5.
2. Blot WJ, Devesa SS, Kneller RW, Fraumeni Jr JF. Rising incidence of adenocarcinoma of the esophagus and gastric cardia. Jama. 1991;265:1287–9.
3. Deans C, Yeo MS, Soe MY, Shabbir A, Ti TK, So JB. Cancer of the gastric cardia is rising in incidence in an Asian population and is associated with adverse outcome. World J Surg. 2011;35:617–24.
4. Okholm C, Svendsen LB, Achiam MP. Status and prognosis of lymph node metastasis in patients with cardia cancer—a systematic review. Surg Oncol. 2014;23:140–6.
5. Schuhmacher C, Gretschel S, Lordick F, Reichardt P, Hohenberger W, Eisenberger CF, et al. Neoadjuvant chemotherapy compared with surgery alone for locally advanced cancer of the stomach and cardia: European organisation for research and treatment of cancer randomized trial 40954. J Clin Oncol. 2010;28:5210–8.
6. Gao SG, Wang LD, Feng XS, Ma BG, Wang QM, Guo RF, et al. Expression of p53 and PCNA in intestinal metaplasia tissue adjacent to gastric cardia adenocarcinoma and in gastric cardia biopsy tissue. J Zhengzhou University . 2006;1:30–2.
7. Carr JS, Zafar SF, Saba N, Khuri FR, El-Rayes BF. Risk factors for rising incidence of esophageal and gastric cardia adenocarcinoma. J Gastrointest Cancer. 2013;44:143–51.
8. Lee YY, Derakhshan MH. Environmental and lifestyle risk factors of gastric cancer. Arch Iran Med. 2013;16:358–65.
9. Ameres SL, Zamore PD. Diversifying microRNA sequence and function. Nat Rev Mol Cell Biol. 2013;14:475–88.
10. Bartel DP. MicroRNAs: target recognition and regulatory functions. Cell. 2009;136:215–33.
11. Ghahhari NM, Babashah S. Interplay between microRNAs and wnt/beta-catenin signalling pathway regulates epithelial-mesenchymal transition in cancer. Eur J Cancer. 2015;51:1638–49.
12. Xiong H, Li Q, Liu S, Wang F, Xiong Z, Chen J, et al. Integrated microRNA and mRNA transcriptome sequencing reveals the potential roles of miRNAs in stage i endometrioid endometrial carcinoma. PLoS One. 2014;9, e110163.
13. Chawla JP, Iyer N, Soodan KS, Sharma A, Khurana SK, Priyadarshni P. Role of miRNA in cancer diagnosis, prognosis, therapy and regulation of its expression by epstein-barr virus and human papillomaviruses: with special reference to oral cancer. Oral Oncol. 2015;51:731–7.
14. Barger JF, Nana-Sinkam SP. MicroRNA as tools and therapeutics in lung cancer. Respir Med. 2015;109:803–12.
15. Zaravinos A. The regulatory role of microRNAs in emt and cancer. J Oncol. 2015;2015:865816.
16. Oh HK, Tan AL, Das K, Ooi CH, Deng NT, Tan IB, et al. Genomic loss of mir-486 regulates tumor progression and the olfm4 antiapoptotic factor in gastric cancer. Clin Cancer Res. 2011;17: 2657–67.
17. Tseng CW, Lin CC, Chen CN, Huang HC, Juan HF. Integrative network analysis reveals active microRNAs and their functions in gastric cancer. BMC Syst Biol. 2011;5:99.
18. Wang Y, Feng X, Jia R, Liu G, Zhang M, Fan D, et al. Microarray expression profile analysis of long non-coding RNAs of advanced stage human gastric cardia adenocarcinoma. Mol Genet Genomics. 2014;289:291–302.
19. Chen Z, Ma T, Huang C, Zhang L, Xu T, Hu T, et al. MicroRNA-148a: a potential therapeutic target for cancer. Gene. 2014;533:456–7.
20. Huang F, Tang J, Zhuang X, Zhuang Y, Cheng W, Chen W, et al. Mir-196a promotes pancreatic cancer progression by targeting nuclear factor kappa-b-inhibitor alpha. PLoS One. 2014;9, e87897.
21. Calvano Filho CM, Calvano-Mendes DC, Carvalho KC, Maciel GA, Ricci MD, Torres AP, et al. Triple-negative and luminal a breast tumors: differential expression of mir-18a-5p, mir-17-5p, and mir-20a-5p. Tumour Biol. 2014;35:7733–41.
22. Zheng Q, Ye J, Cao J. Translational regulator eif2alpha in tumor. Tumour Biol. 2014;35:6255–64.
23. Stolboushkina EA, Garber MB. Eukaryotic type translation initiation factor 2: structure-functional aspects. Biochemistry Biokhimiia. 2011;76:283–94.
24. Lu PD, Jousse C, Marciniak SJ, Zhang Y, Novoa I, Scheuner D, et al. Cytoprotection by pre-emptive conditional phosphorylation of translation initiation factor 2. EMBO J. 2004;23:169–79.
25. Harris AL. Hypoxia—a key regulatory factor in tumour growth. Nat Rev Cancer. 2002;2:38–47.
26. Aktas BH, Qiao Y, Ozdelen E, Schubert R, Sevinc S, Harbinski F, et al. Small-molecule targeting of translation initiation for cancer therapy. Oncotarget. 2013;4:1606–17.
27. Liu P, Cheng H, Roberts TM, Zhao JJ. Targeting the phosphoinositide 3-kinase pathway in cancer. Nat Rev Drug Discov. 2009;8:627–44.
28. Jain RK. Normalization of tumor vasculature: an emerging concept in antiangiogenic therapy. Science. 2005;307:58–62.
29. Wander SA, Hennessy BT, Slingerland JM. Next-generation mTOR inhibitors in clinical oncology: how pathway complexity informs therapeutic strategy. J Clin Invest. 2011;121:1231–41.
30. Royce ME, Osman D. Everolimus in the treatment of metastatic breast cancer. Breast Cancer. 2015;9:73–9.
31. Iyer G, Hanrahan AJ, Milowsky MI, Al-Ahmadie H, Scott SN, Janakiraman M, et al. Genome sequencing identifies a basis for everolimus sensitivity. Science. 2012;338:221.
32. Tan X, Liu Y, Hou J, Cao G. Targeted therapies for renal cell carcinoma in Chinese patients: focus on everolimus. Onco Targets Therapy. 2015;8:313–21.
33. Guan Y, Mizoguchi M, Yoshimoto K, Hata N, Shono T, Suzuki SO, et al. Mirna-196 is upregulated in glioblastoma but not in anaplastic astrocytoma and has prognostic significance. Clin Cancer Res. 2010;16:4289–97.
34. Lu YC, Chang JT, Liao CT, Kang CJ, Huang SF, Chen IH, et al. Oncomir-196 promotes an invasive phenotype in oral cancer through the nme4-jnk-timp1-mmp signaling pathway. Mol Cancer. 2014;13:218.
35. Candini O, Spano C, Murgia A, Grisendi G, Veronesi E, Piccinno MS, et al. Mesenchymal progenitors aging highlights a mir-196

switch targeting hoxb7 as master regulator of proliferation and osteogenesis. Stem Cells. 2015;33:939–50.
36. Yang G, Han D, Chen X, Zhang D, Wang L, Shi C, et al. Mir-196a exerts its oncogenic effect in glioblastoma multiforme by inhibition of IkappaBalpha both in vitro and in vivo. Neuro-Oncology. 2014;16:652–61.
37. Sand M, Skrygan M, Sand D, Georgas D, Hahn SA, Gambichler T, et al. Expression of microRNAs in basal cell carcinoma. Br J Dermatol. 2012;167:847–55.
38. Pena-Chilet M, Martinez MT, Perez-Fidalgo JA, Peiro-Chova L, Oltra SS, Tormo E, et al. MicroRNA profile in very young women with breast cancer. BMC Cancer. 2014;14:529.
39. Wang B, Li J, Sun M, Sun L, Zhang X. MiRNA expression in breast cancer varies with lymph node metastasis and other clinicopathologic features. IUBMB life. 2014;66:371–7.
40. Rossi M, Kilpinen H, Muona M, Surakka I, Ingle C, Lahtinen J, et al. Allele-specific regulation of disc1 expression by mir-135b-5p. Eur J Hum Genet. 2014;22:840–3.
41. Song Y, Li L, Ou Y, Gao Z, Li E, Li X, et al. Identification of genomic alterations in oesophageal squamous cell cancer. Nature. 2014;509:91–5.